Turkish Journal of Electrical Engineering & Computer Sciences

http://journals.tubitak.gov.tr/elektrik/

Research Article

Turk J Elec Eng & Comp Sci
(2016) 24: 3597 – 3608

doi:10.3906/elk-1504-59

Pure fuzzy Hall effect sensors for permanent magnet synchronous motor

İbrahim ALIŞKAN[1,*], **Rüstem YILMAZEL**[2]

[1]Department of Electrical and Electronics Engineering, Bülent Ecevit University, Zonguldak, Turkey
[2]Department of Electronics and Automation, Kırıkkale University, Kırıkkale, Turkey

Received: 07.04.2015 • **Accepted/Published Online:** 20.05.2015 • **Final Version:** 20.06.2016

Abstract: An investigation about Hall effect sensors' efficiency is confirmed in permanent magnet synchronous motor (PMSM) drive systems. A fuzzy control algorithm is used as an artificial intelligence controller. Large scale and low slopes are used for creating membership functions and a sensitive controller is obtained. Speed is wanted to be taken under control and a minimum error value is aimed. PMSM drive systems are established using MATLAB-Simulink/SimPower. Simulations are realized with real-time parameters in discrete mode. A fuzzy logic controller is designed by using the MATLAB/Fuzzy Logic Toolbox. A normalization technique and high resolution output of the fuzzy logic controller (FLC) are unique aspects of the work. Input variable bandwidths are narrowed and the number of membership functions is reduced. The taken steps provide positive effects against variation of input parameters. Finally, sharp impacts are not produced by the fuzzy controller. Results verified that the Hall effect supported controller system gives better results than sensorless one. This is especially observed at change points of reference speed. Low complitude oscillations and short settling time are achieved on speed and torque signals.

Key words: Permanent magnet synchronous motor, fuzzy logic, artificial intelligence, power electronics, discrete time systems

1. Introduction

Synchronous motors are double excitation machines and they rotate at synchronous speed, which depends on source frequency and number of motor poles. The supply voltage has the same frequency as the mechanical motor speed for a synchronous motor. The stator of the motor is fed by an alternative current, whereas the rotor is fed by direct current. Permanent magnets are placed at the rotor and provide a rotor magnetic field. Therefore, there is no need for a second source and a permanent magnet synchronous motor (PMSM) is made [1].

There are many advantages of PMSMs as compared with other types of electrical machines. For example, high efficiency, high torque to inertia ratio, high torque to volume ratio, high air gap flux density, high power factor, and high acceleration and deceleration rates can be mentioned [2]. The PMSM is used in different types of applications such as air conditioner compressors, direct-drive washing machines, refrigerator compressors, and automotive air conditioner compressors [3]. It can be designed in a smaller size than other machines and equal power values are produced [4].

Like other machines, PMSM mechanical parameters, torque and/or speed, must be taken under control.

*Correspondence: ialiskan@beun.edu.tr

High efficiency is obtained by using controllers that are based on artificial intelligence. The fuzzy controller may be the best known type of controller in this group [5,6].

We want to achieve a low speed error with load torque equal to the mechanical output torque of a PMSM. Feedback signals are needed for closed loop control algorithms [7,8]. Mechanical speed is the main feedback signal for us. The signal is generally used for motor controllers [9,10].

Drive system simulations are confirmed using MATLAB/Simulink. A unique FLC is designed and used for comparison analysis. We use a mathematical model of the PMSM for constituting the d-q axis reference current for sensorless control operation. The aims of the drive system are to have speed control at wide speed bandwidth and torque stability. Simulation results verified that the speed controller, which is a FLC, attains the wanted dynamic response.

Normalization and denormalization have important effects on FLC performance. Thus, input values are taken into –1 ... 1 bandwidth. After this, membership functions are admitted to the process. If we look at FLC output, the value can move from –1 to 1. The denormalization value is selected as satisfying the PMSM maximum supply voltage value or maximum i_q. Torque and speed stabilities are obtained and Hall effect sensors' positive effects are proved.

2. PMSM modeling

A mathematical model of the PMSM has been developed by making some assumptions [11,12]. These are:

- Saturation is overlooked.
- The induced EMF is sinusoidal.
- Hysteresis losses are negligible.

Equations related to voltage are given in Eqs. (1) and (2).

$$V_q = R_s i_q + \omega_r \lambda_d + \rho \lambda_q \tag{1}$$

$$V_d = R_s i_d - \omega_r \lambda_q + \rho \lambda_d \tag{2}$$

Eqs. (3) and (4) provide the flux linkages.

$$\lambda_q = L_q i_q \tag{3}$$

$$\lambda_d = L_d i_d + \lambda_f \tag{4}$$

The dq axis voltage equations, Eq. (5) and Eq. (6), are obtained by substituting Eq. (3) and Eq. (4) into Eq. (1) and Eq. (2).

$$V_q = R_s i_q + \omega_r (L_d i_d + \lambda_f) + \rho L_q i_q \tag{5}$$

$$V_d = R_s i_d - \omega_r L_q i_q + \rho (L_d i_d + \lambda_f) \tag{6}$$

The mechanical torque equation is given in Eq. (7).

$$T_e = T_L + B\omega_m + J\frac{d\omega_m}{dt} \tag{7}$$

If Eq. (7) is used for angular velocity, Eq. (8) can be attained. The mechanical speed of the rotor is formulized by Eq. (9).

$$\omega_m = \int (\frac{T_e - T_L - B\omega_m}{J})dt \tag{8}$$

$$\omega_m = \omega_r \left(\frac{2}{P}\right) \tag{9}$$

Here V_q and i_q are the q-axis voltage and current. V_d and i_d are the d-axis voltage and current. L_q and L_d are the q-axis and d-axis self-inductance. L_q and L_d have variations at dynamic loading conditions and different steady-state positions [13]. R_s is stator resistance. ω_r and ω_m are electrical and rotor speeds. λ_d and λ_q are flux linkage due to the d-axis and q-axis. ρ is the derivative operator. λ_f is the field flux linkage. T_e is the electromagnetic torque. P is the number of poles and B is the friction constant. T_L is the load torque and J is inertia.

3. PMSM drive systems

Rotor position is very significant for PMSM drive systems. The value is a necessity, because the stator current vector is directed using position information. This position is shown for both sensor-based control and sensorless control [14].

4. Hall effect sensor supported control for a PMSM

Figure 1 summarizes the proposed controller system. Sensors are used to get the information of rotor position and thus the control design becomes simpler. This control method is cheap for low-cost applications [15].

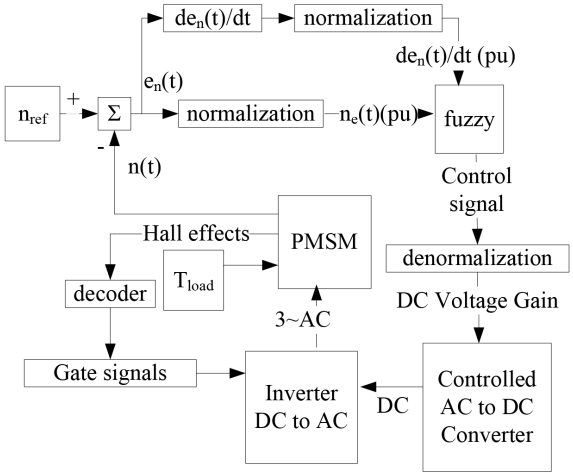

Figure 1. Controller system with Hall effect sensors.

Information is received from Hall effect sensors and entered to the decoder. The signals, received from the output of the decoder, go to the gate signal generator. The output of the gates enters the universal bridge for triggering. The signals that are obtained from the output of the FLC go to the controlled voltage source. The error signal is equal to a difference value, which is taken from a subtraction operation between the reference speed and feedback speed. The time axis is used for error signal derivation. Sampling time is enough for

slope calculation. Both of the parameters are given as inputs to the FLC. The universal bridge consists of MOSFET/diodes. To drive the PMSM, armature phase signals are generated in the universal bridge. For this simulation the fundamental sample time is 10 μs. A discrete solver is selected here [16].

5. Sensorless control for a PMSM

The control algorithm and signal routing are shown in Figure 2. Rotor angle and stator current information are enough for this control technique. The main advantages of this technique are faster response and lower cost [11]. The rotor angle, theta-mechanic, is received from the PMSM and the signal, which is produced by the controller, is given to the PWM inverter as a reference signal. Reference signals and stator current signals that are received from the PMSM are compared to each other. To drive the PMSM, output signals of the PWM inverter are given to the PMSM as supporter alternative current signals. The classic saw tooth signal, with pulse width modulation, is enough for driver signals [17].

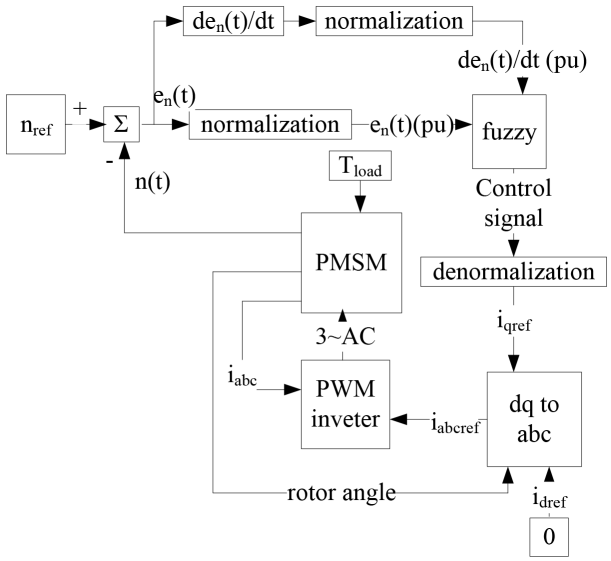

Figure 2. Sensorless controller diagram.

6. FLC structure

Fuzzy logic is an artificial intelligence theory. A human approach is used for the solution of different problems and there is no need for mathematical theory. The FLC is designed as an alternative according to traditional control methods for making better control results when complex systems are wanted to be controlled. The algorithm allows direct user inputs and benefits from the experiences of the user. In addition, easy and cheap controllers can be obtained for systems that are not modeled by using mathematical algorithms [18]. Now such an algorithm is going to be applied for the design steps.

Figure 3 shows the fundamental form of the controller. There are a few main stages to design a FLC.

- The first step is the definition of input and output variables.
- The second step is decision making of fuzzy control rules.
- Fuzzy logic inference is made.
- Finally, defuzzification and aggregation are done [5,6].

Important components of fuzzy logic will be instituted in this concept.

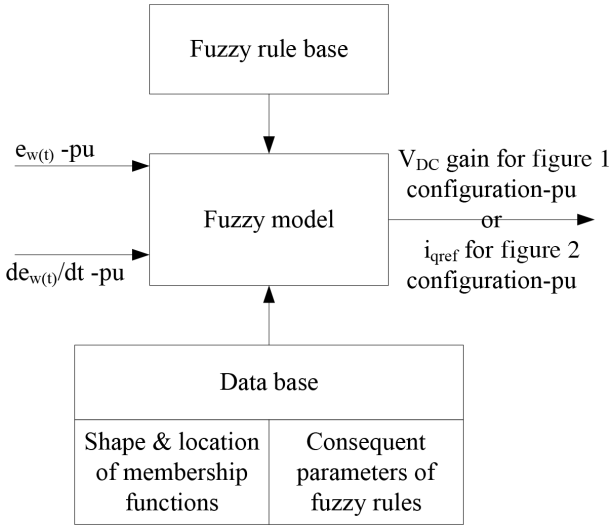

Figure 3. Links of components of Mamdani type fuzzy controller [6].

6.1. Membership functions

The first step is definition of input and output variables. The cycle of the rotor is the main parameter and it is needed for control. Error of the parameter ($e_{n(t)}$) and its slope ($de_{n(t)}/dt$) are enough for guidance of output. Mathematical definitions of these are listed in Eqs. (10) and (11).

Both of the inputs must be taken into the 0 ... 1 range and normalization is used for this reason. Adaptive or constant parameters may be used in normalization as given in Eq. (12). Saturation values of ± 2 and 0.125 gain are used for speed error. The sensitivity of the PMSM is considered and a narrow area with low slope membership functions, shown in Figures 4 and 5, can be obtained in this way. The maximum slope value goes to infinity theoretically. α, 89.999° <90° , is an appropriate angular position. Tangent α is used for both saturation values and gain value.

$$e_{n(t)} = n(t+\tau) - n(t) \tag{10}$$

$$\frac{de_{n(t)}}{dt} = \frac{e_{n(t+\tau)} - e_{n(t)}}{\tau} \tag{11}$$

$$pu = \frac{measurementvalue}{\max valueofparameter}, pu : perunit. \tag{12}$$

Here, τ is the sampling time of simulations [16].

Controller inputs are made by Eqs. (10) and (11). The inputs are processed by membership functions.

The input variable has an effective role in the –0.25 ... 0.25 range, because ± 2 saturation values and 0.125 normalization gain are used.

For input-2, the saturation values and normalization value are equal to each other at the same amplitude value and in this way, the –1 ... 1 range is taken in the active zone. However, derivation causes an impulse at the FLC output. This must be prevented and positions of membership functions that are placed in Figure 5 are assigned using this object.

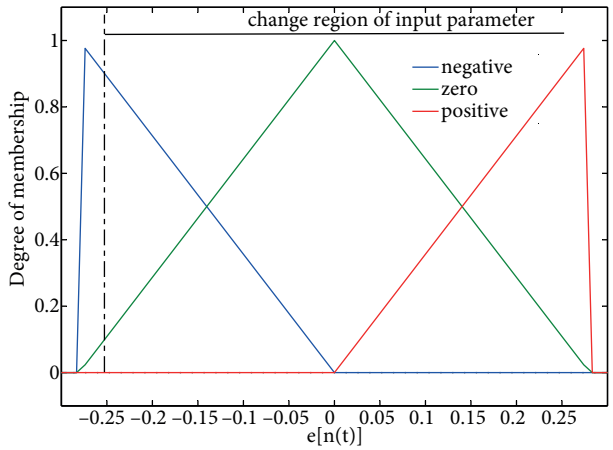

Figure 4. Low slopes and reduced memberships for speed error.

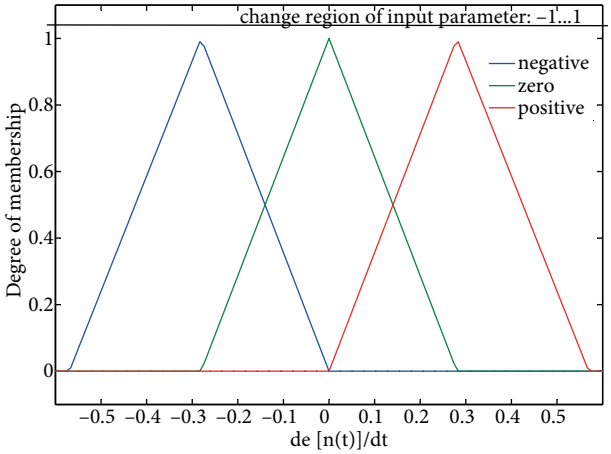

Figure 5. Normal slopes and reduced memberships for derivation of speed error.

We need to use the 0 ... 1 range for output, because negative signals will not be used for reference i_q current or reference V_{DC} voltage. On the other hand, we know that the PMSM is a sensitive machine and sharp signal changes will reverberate to mechanical outputs. As seen in Figure 6, a large scale and –1 ... 1 saturation points are enough for the wanted conditions. If we look at Table 1, all membership functions are used and their low slope values are derived with this method.

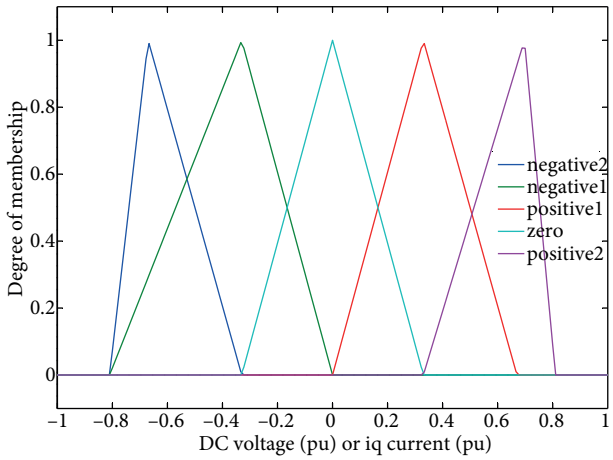

Figure 6. Output memberships of Mamdani type fuzzy controller.

Table 1. FLC rule base matrix.

$(d/dt)e_{n(t)}$ / $e_{n(t)}$	negative	zero	positive
negative	negative2	negative2	positive1
zero	zero	zero	zero
positive	negative1	positive2	postive1

7. Rule base

Inputs and outputs are connected to each other using the rule base, which is given in Table 1. Output of the fuzzy controller is formed by evaluation of inputs. The structure of the rule base is created using IF-THEN conditions [19].

$$\begin{aligned} &IFinput-1=membershipfunction(k_1)\\ &andinput-2=membershipfunction(k_2)\\ &THENouput=membershipfunction(k_3) \end{aligned} \tag{13}$$

k_1, k_2, and k_3 indicate related variable functions, as the zero function of e[n(t)].

The 'IF' part of the rule is a reference to the membership degree of the input part of fuzzy sets. 'THEN' is a reference to output. The size of the rule matrix is equal to m $\times$ n. m and n are the number of functions of input-1 and input-2.

Elementary and effective artificial systems may be uploaded into 16-bit processor units. A minimum number of functions and a low size (3 $\times$ 3) rule base matrix are produced here.

8. Output surface

The rule base and the functions produce a set of output values and the input-1 – input-2 – output (x – y – z) axis is used for a graphical presentation. The control signal routing is called the surface and is given in Figure 7. The maximum value is equal to 0.47 (yellow) and the minimum value is –0.47 (blue). The colorless region of the surface means a zero value. Classic $\pm$ 1 margins are not obtained here, because we do not want to get a sharp change at signal rotation.

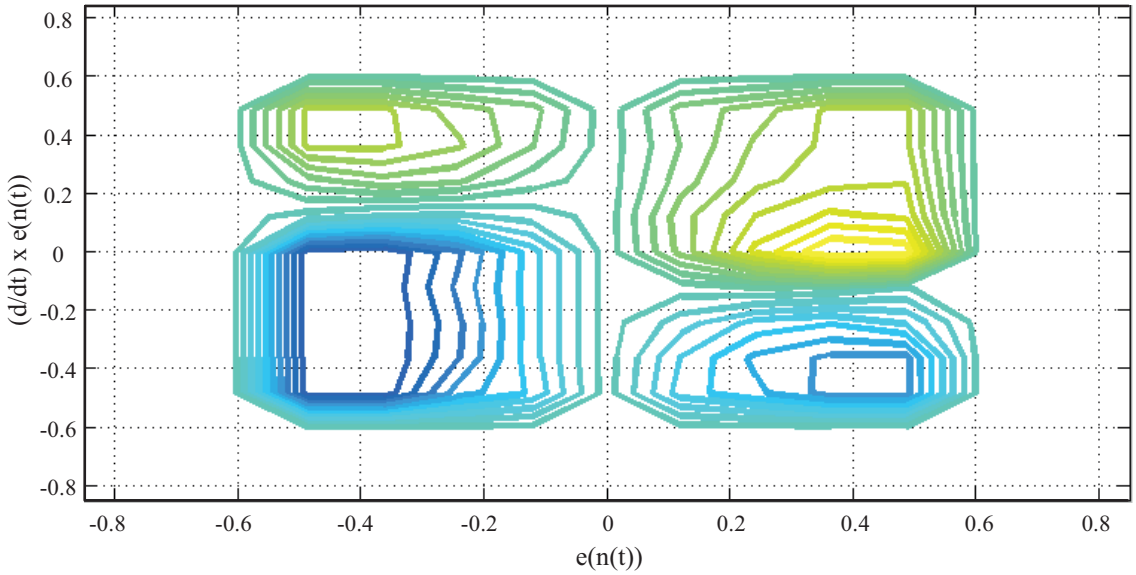

Figure 7. Output surface of FLC.

9. Denormalization for outputs

The FLC provides us with pu values that must be transformed to the gain of system parameter. As an example, the output must be transformed to an i_q signal value for sensorless control.

If we think about the control system, which uses Hall effect sensors, the output must be transformed to V_{DC} gain. As is known, the nominal DC voltage value for the PMSM is equal to 300 V and the maximum gain value of the output of the FLC is equal to 0.47 peak. Eq. (14) is used for solution of the parametric transformation:

$$denormalizationcoefficient = 300/0.47 \tag{14}$$

If Hall effect sensors are not used, we can notice that the controller output means the i_q reference signal. An experimental working is confirmed at the nominal values given in Table 2, where 300 V is DC support voltage and 8 Nm is load torque.

Table 2. PMSM parameters.

Parameter	Value
DC supply voltage-V_{DC}	300 V
Nominal load-T_n	8 Nm
Nominal speed-n_s	2000 rpm
Inertia-J	0.0006329 kgm^2
Viscous damping-B	0.0003035 Nms
Number of pole pairs-p	4
Stator phase resistance-R_s	0.9585 Ω
Armature inductance-L_s	5.25 mH
Flux linkage-λ_f	0.1827 Vs

The current movement is given in Figure 8 and the stable state value of i_q is equal to nearly 7 A. The maximum gain value is 55.68 A, which belongs to a transient time region. If we look at the current from this side, Eq. (15) can be employed for parametric transformation:

$$denormalizationcoefficient = i_{q\max} * 0.47 \tag{15}$$

When the coefficient and the output are used in multiplication, a 12.3 A peak current value emerges.

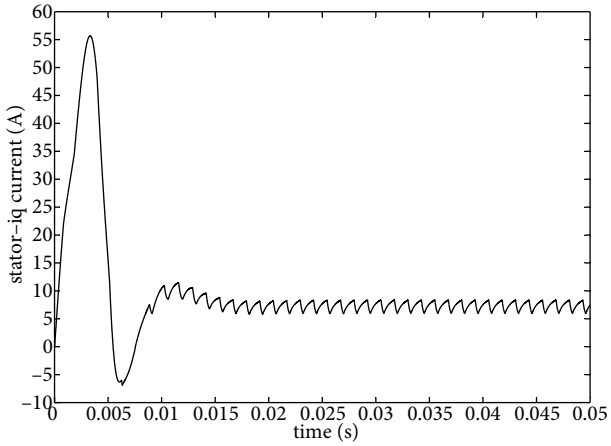

Figure 8. $i_q(t)$ at nominal mechanic values.

PMSM stator windings are protected against thermal effects and the starting operation is taken into a narrow oscillation range.

10. Results

Simulation diagrams of the system for the PMSM are given in Figures 1 and 2. Variable speed reference and different load conditions are used for evaluation of the controller performance. Aims of the FLC are minimum values for stable state errors and for short settling times for mechanical parameters. First of all, mechanical speeds given in Figure 9 are considered and stable state error (e_{ss}) with settling time (τ_s) are evaluated by using Figure 10. Fast response and about zero overshoot can be indicated for both of the controllers. If we want to identify numerical values, the 0 ... 0.05 s time range may be used. When a sensorless controller is used, the overshoot value goes to zero, but ˜8 rpm, equal to 1.6% of reference speed, is done by the Hall effect supported controller system. Meanwhile, τ_s values are 10 ms for the sensor-based controller and ˜17 ms for the sensorless controller. If steady state rotor speed is taken into consideration, Eq. (16) will be explanatory about this subject.

$$e_{ss} = \frac{n_{reference} - n_{rotor}}{n_{reference}} \cdot 100\% \tag{16}$$

Here, the e_{ss} value is 0.1% of reference speed for the sensor-based controller and is 0.2% for the sensorless controller system. Success of the sensor-based controller is noticed and stable state error value is reduced to half of the sensorless controller performance value. Oscillation margins of the speed, ± 0.5 rpm and ± 1.1 rpm, satisfy a better performance of the Hall effect supported controller.

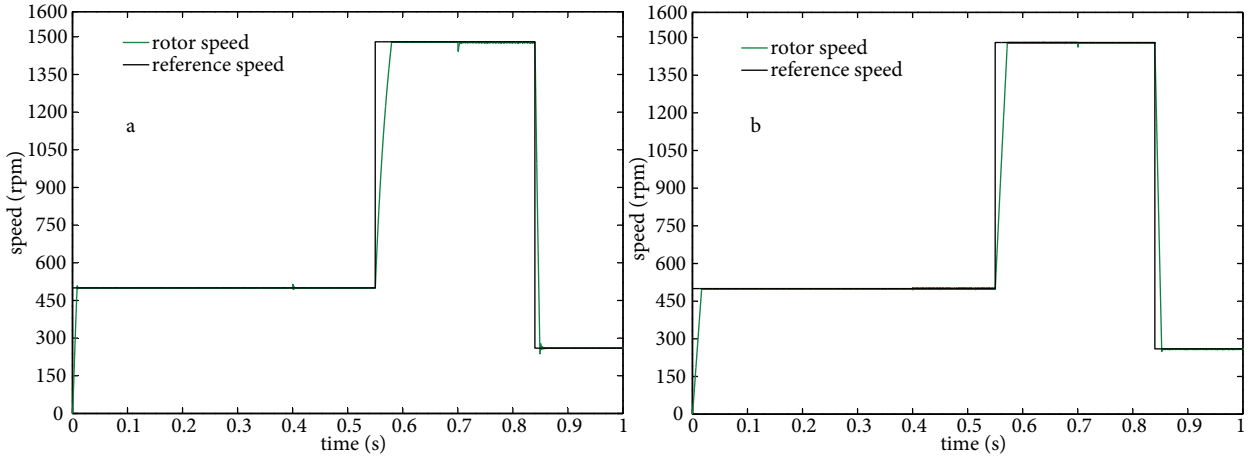

Figure 9. Obtained rotor speed positions by Hall effect supported controller and sensorless controller in time domain, respectively.

Motor load is very important because we want to work at different operation points. If we look at Figure 11, different loads can be found in the time domain. Mechanical torque of the rotor is given by Eq. (7). Obtained results show that Hall effect sensors have an important effect on output torque of the PMSM because oscillation margins are ± 0.1 Nm for the sensor-based controller and ± 0.405 Nm for the other controller.

Another object of the controllers is that the $i_q \leq i_{qnominal}$ condition must be provided. Figure 12 illustrates this subject. Both of the controllers arrive at the aim, but smaller oscillation margins and lower peak values are presented by the sensor-based controller. This one is supported with using a 0–0.4 s time range and values that are ± 0.5 A and ± 2 A.

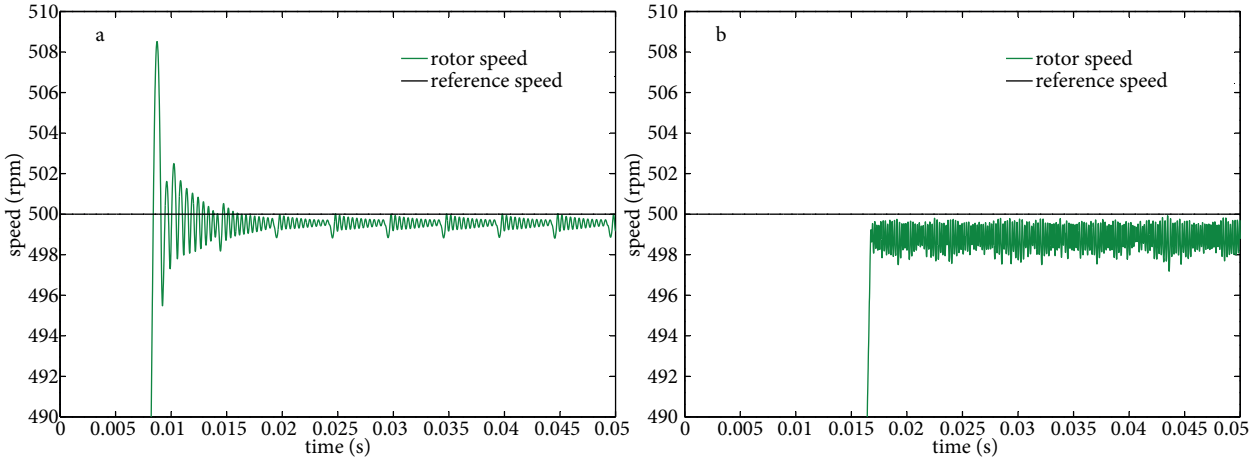

Figure 10. Mechanical speeds reached by sensor-based and sensorless controllers in the 0–0.05 s time range, respectively.

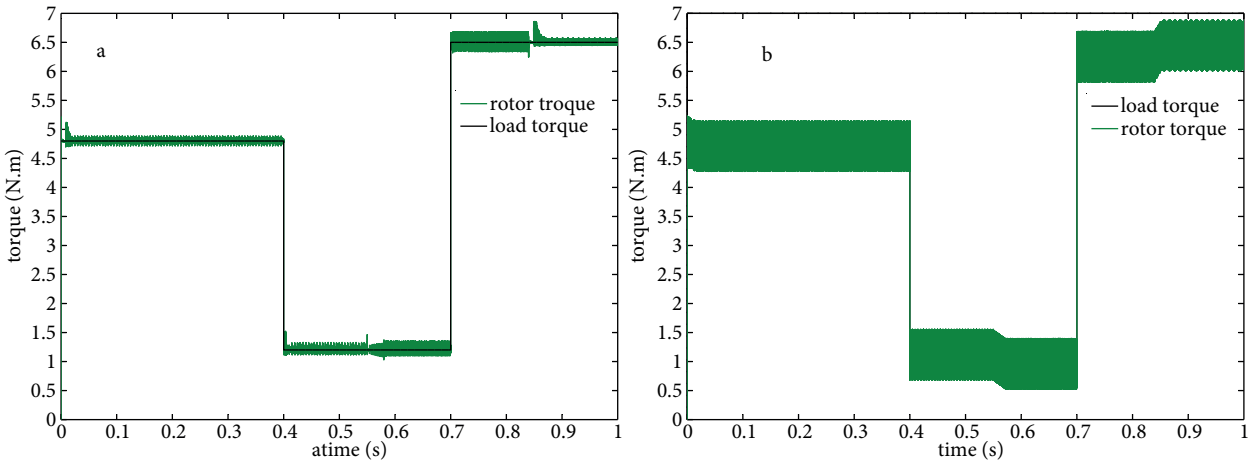

Figure 11. Torque positions of PMSM; the second one is obtained by the sensorless controller.

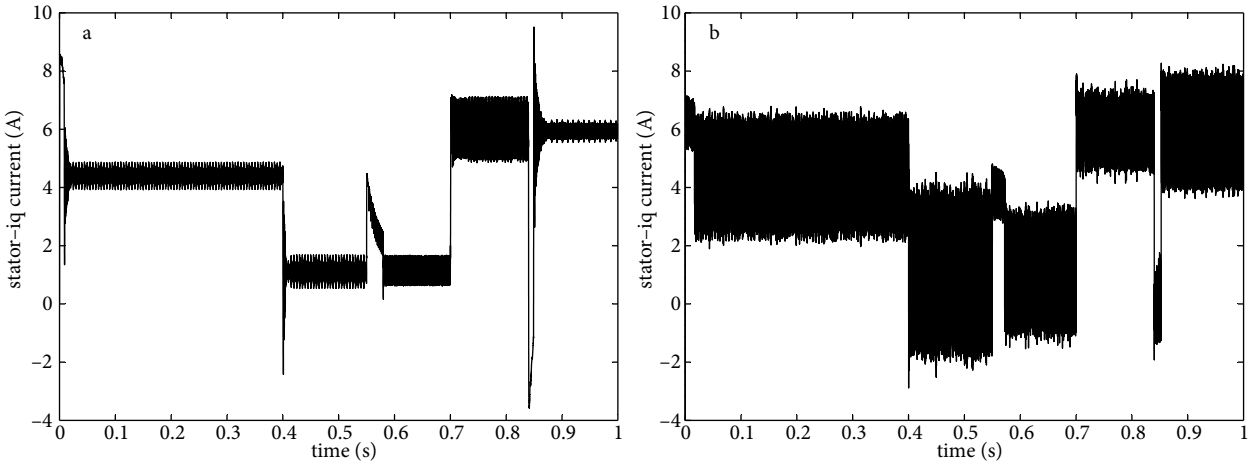

Figure 12. i_q positions in time domain; the first one is obtained by sensor supported FLC.

The last parameter that must be considered is the output signal of the controllers. Stability of the controllers is shown in Figure 13. Variation of load and variation of reference speed show their effects on the

controller signals, and 0.4 s is an example point for load variation and 0.55 s is given as an example for reference speed variation point. More stable signals are obtained by the Hall effect supported system. This is seen at oscillation margins and output gain.

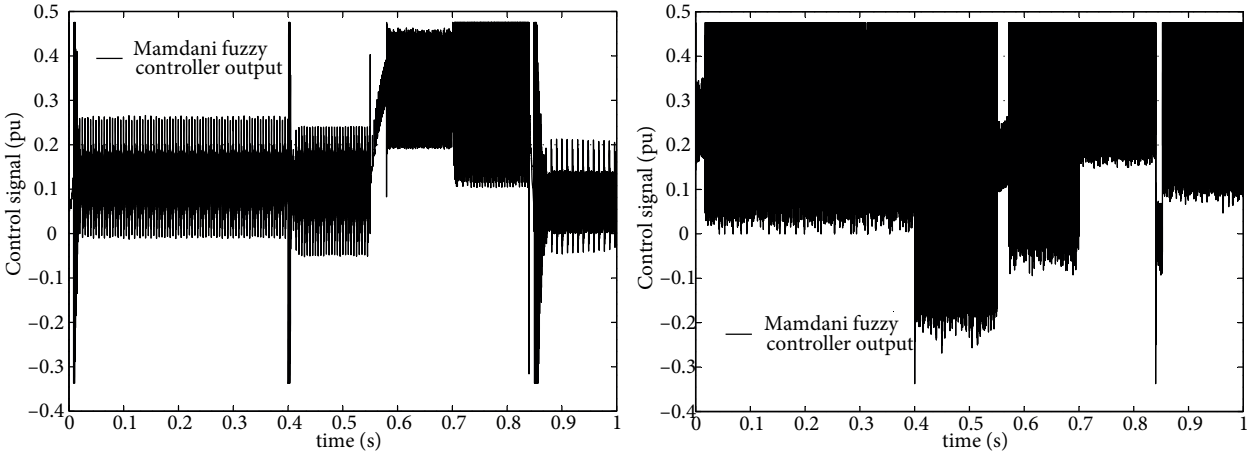

Figure 13. FLC outputs; the first one is taken from system including Hall effects.

All positive effects of the sensors are as given in [20]. A cheap control system and small error values of the output parameters are clearly seen.

11. Conclusion

If a comparison is done about speed performance, positive effects of Hall effect sensors can be shown. Both of the controllers have successful results. We notice that the designed FLC controls the motor under different feedback conditions. The sensor-based controller has faster response than the sensorless controller. The sensorless controller is slower than the other because stator currents are formed by the magnetic field and a delay time emerges during this formation. If speed and overshoot are very important, sensorless drive systems can be used in applications, but oscillation margins and torque errors must be considered. Meanwhile, transient time is very short and e_{ss} values are smaller if a sensor-based drive system is used. All graphs and values display the positive effects of Hall effect sensors.

A discrete simulation technique was used for both systems. As is known, processor units work in discrete mode and because of this developed systems can be realized easily.

Artificial intelligence-based systems achieve results nearly equal to the reference. The reason for this is that they work as the human brain with the desire of a person to reach a target. However, it should not be forgotten that people have different ideas from others and different feelings.

References

[1] Pillay P, Krishnan R. Modeling, simulation and analysis of permanent-magnet motor drives. IEEE T Ind Appl 1989; 25: 265-273.

[2] Qian J, Rahman MA. Analysis of field oriented control for permanent magnet hysteresis synchronous motors. IEEE T Ind Appl 1993; 29: 1156-1163.

[3] Stefanovic VR. Trends in AC drive applications. Elektronika 2006; 10: 10-15.

[4] Sabastial T, Slemon GR, Rahman MA. Modeling of permanent magnet synchronous motors. IEEE T Magn 1986; 22: 1069-1071.

[5] Ross TJ. Fuzzy Logic with Engineering Applications. New York, NY, USA: McGraw-Hill, 1995.

[6] Farinwata SS, Filev D, Langari R. Fuzzy Control Synthesis and Analysis. New York, NY, USA: Wiley, 2000.

[7] Ogata K. Modern Control Engineering. Upper Saddle River, NJ, USA: Prentice Hall, 2002.

[8] Tewari A. Modern Control Design with MATLAB and Simulink. Chichester, UK: John Wiley, 2005.

[9] Aliskan I, Gulez K, Tuna G, Mumcu TV, Altun Y. Nonlinear speed controller supported by direct torque control algorithm and space vector modulation for induction motors in electrical vehicles. Elektron Electrotech 2013; 19: 41-46.

[10] Litcanu M, Andea P, Mihai FIF. Fuzzy logic controller for permanent magnet synchronous machines. In: IEEE 13th International Symposium on Applied Machine Intelligence and Informatics; 22–24 January 2015; Herlany, Slovakia. pp 261-265.

[11] Kamala CK, Paranjothi SR, Paramasivam S. Optimal control of switched reluctance motor using tuned fuzzy logic control. European Journal of Scientific Research 2011; 55: 436-443.

[12] Arroyo ELC. Modeling and simulation of permanent magnet synchronous motor drive system. MSc, University of Puerto Rico, Mayaguez, Puerto Rico, 2006.

[13] Rahman MA, Zhou P. Field circuit analysis of brushless permanent magnet synchronous motors. IEEE T Ind Electron 1996; 43: 256-267.

[14] Chakraborty M. Comparative analysis of speed control of PMSM using PI-controller and fuzzy controller. International Journal of Scientific & Engineering Research 2013; 4: 103-108.

[15] Heydari F, Sheikholeslami A, Firouzjah KG, Lesan S. Predictive field-oriented control of PMSM with space vector modulation technique. Frontiers of Electrical and Electronics Engineering 2010; 5: 91-99.

[16] Ogata K. Discrete-Time Control Systems. Upper Saddle River, NJ, USA: Prentice Hall, 1995.

[17] Mohan N, Undeland TM, Robbins WP. Power Electronics. New York, NY, USA: Wiley, 1995.

[18] Gupta JB. Theory and Performance of Electrical Machines. New Delhi, India: S.K. Kataria & Sons Publishing, 2013.

[19] Karray FO, Silva CD. Soft Computing and Intelligent Systems Design Theory. Essex, UK: Addison Wesley, 2004.

[20] Ozturk SB, Akin B, Toliat HA, Ashrafzadeh F. Low-cost direct torque control of permanent magnet synchronous motor using Hall-effect sensors. In: IEEE 2006 Applied Power Electronics Conference and Exposition; 19–23 March 2006; Texas, USA. pp. 667-673.